

MULTIWAVELENGTH OBSERVATIONS OF THE HOT DB STAR PG 0112+104¹

P. DUFOUR², S. DESHARNAIS², F. WESEMAEL², P. CHAYER³, T. LANZ⁴, P. BERGERON², G. FONTAINE², A. BEAUCHAMP^{2,5},
R.A. SAFFER⁶, J.W. KRUK⁷, M.-M. LIMOGES²

Submitted to The Astrophysical Journal

ABSTRACT

We present a comprehensive multiwavelength analysis of the hot DB white dwarf PG 0112+104. Our analysis relies on newly-acquired FUSE observations, on medium-resolution FOS and GHRS data, on archival high-resolution GHRS observations, on optical spectrophotometry both in the blue and around H α , as well as on time-resolved photometry. From the optical data, we derive a self-consistent effective temperature of $31,300 \pm 500$ K, a surface gravity of $\log g = 7.8 \pm 0.1$ ($M = 0.52 M_{\odot}$), and a hydrogen abundance of $\log N(\text{H})/N(\text{He}) < -4.0$. The FUSE spectra reveal the presence of C II and C III lines that complement the previous detection of C II transitions with the GHRS. The improved carbon abundance in this hot object is $\log N(\text{C})/N(\text{He}) = -6.15 \pm 0.23$. No photospheric features associated with other heavy elements are detected. We reconsider the role of PG 0112+104 in the definition of the blue edge of the V777 Her instability strip in light of our high-speed photometry, and contrast our results with those of previous observations carried out at the McDonald Observatory.

Subject headings: white dwarfs

1. ASTROPHYSICAL CONTEXT

The DB stars constitute the subgroup of helium-atmosphere white dwarfs whose optical spectrum is dominated by the transitions of neutral helium. Their effective temperatures extend from roughly 13,000 K upward to $\sim 40,000$. The lower boundary is imposed by the visibility of the He I lines, that become very weak and disappear near that effective temperature, while the upper boundary is the effective temperature near which the smooth merging occurs between the DB sequence and the sequence of the hotter DO stars, whose spectrum is characterized by lines of ionized helium. Some filling-in of the region between 30,000 K and 40,000 K, previously thought to be devoid of helium-atmosphere white dwarfs (Wesemael et al. 1985) and known as the “DB gap” (Liebert et al. 1987), has been accomplished with the recent observation by Eisenstein et al. (2006)

of several fainter hot DB stars in the Sloan Digital Sky Survey (SDSS).

While the idea of a true gap in the cooling sequence of the helium-atmosphere white dwarfs has now been abandoned, Eisenstein et al. (2006) argue nevertheless for the presence of a residual imbalance in the relative numbers of DA and DB stars, in the sense that the DA/DB number ratio is ~ 2.5 times larger at 30,000 K than it is at 20,000 K. This result is interpreted in terms of a transformation of ~ 10 % of the DA stars observed at 30,000 K into DB stars by the time these objects cool down to 20,000 K. If this were the case, the physical mechanism invoked by Liebert et al. (1987) and Fontaine & Wesemael (1987) within their global spectral evolution scheme for white dwarfs might still be relevant. It would require that a fraction of DA white dwarfs be characterized by a hydrogen envelope that is thin enough (of the order of $M_H < 10^{-14.9} M_{\star}$) for mixing to start between that envelope and the active, underlying helium convection zone. The photospheric composition would thereby revert to a helium-dominated one as the star proceeds along its cooling track.

Before the numerous SDSS discoveries, the northern DB star PG 0112+104 had long held the status of the hottest DB star. Today, it merely appears cooler than most of the SDSS stars. Nevertheless, its discovery in the PG survey at a reasonable brightness ($V \sim 15.4$) makes it accessible to a variety of instruments, a substantial bonus for a hot DB star. As such, it represents the best studied DB white dwarf above 30,000 K. Since it is not exactly understood how DB stars above 30,000 K fit into white dwarf evolution, a comprehensive analysis of PG 0112+104 is crucial for an understanding of the still uncertain nature of the spectral evolution mechanism. PG 0112+104 is also the best object near the uncertain boundaries of the V777 Her variable separating hot DB star from DB pulsators so an accurate determination of its atmospheric parameters is important for an unambiguous empirical location of the blue edge of the

¹ Based on observations with the FUSE satellite, which is operated by the Johns Hopkins University under NASA contract NAS 5-32985; with the NASA/ESA *Hubble Space Telescope*, obtained at the Space Telescope Science Institute, which is operated by the Association of Universities for Research in Astronomy, Inc., under the NASA contract NAS 5-26555; and with the Kitt Peak National Observatory, National Optical Astronomy Observatories, operated by the Association of Universities for Research in Astronomy, Inc., under cooperative agreement with the National Science Foundation.

² Département de Physique, Université de Montréal, C.P. 6128, Succ. Centre-Ville, Montréal, QC H3C 3J7, Canada; dufourpa, stephanie, wesemael, bergeron, fontaine, limoges@astro.umontreal.ca

³ Space Telescope Science Institute, 3700 San Martin Drive, Baltimore, MD 21218, USA; chayer@stsci.edu

⁴ Department of Astronomy, University of Maryland, College Park, MD 20742, USA; lanz@astro.umd.edu

⁵ Forensic Technologies Wai Inc., 5757 Boulevard Cavendish, Montréal, QC H4W 2W8, Canada; alain.beauchamp@ftibis.com

⁶ DataTime Consulting, 109 Forrest Avenue, Narberth, PA 19072, USA; rex.saffer@comcast.net

⁷ Bloomberg Center for Physics and Astronomy, The Johns Hopkins University, Baltimore, MD 21218, USA; kruk@pha.jhu.edu

DB instability strip.

Prompted by these considerations and by FUSE observations secured by one of us (TL), we endeavor here to reexamine PG 0112+104. With the recent demise of FUSE, this object is the last classical DB star for which FUSE data are available and unpublished. These data are combined here with additional, and largely unpublished, information available on this object in order to constrain effectively its atmospheric properties and to try to shed light on its nature. In addition, the status of PG 0112+104 as a non-variable star has recently been challenged (Shipman et al. 2002; Provencal et al. 2003) so we take advantage of this study to reconsider the issue of the variability of this critical object.

We present the observational material on which this investigation is based in § 2, and discuss some issues related to the modeling of DB stars in § 3 and 4. Our reanalysis follows in § 5, while our conclusions are presented in § 6.

2. OBSERVATIONAL MATERIAL

2.1. FUSE data

The FUSE detectors span the ultraviolet region between 905 and 1187 Å, a region where numerous transitions associated with heavy elements are located. The spectroscopic observations of PG 0112+104 were secured in TTAG mode through the high-throughput LWRs aperture, which provides high-resolution ultraviolet spectra with $\lambda/\Delta\lambda \sim 15,000$. One set of exposures, 22.9 ks long, was secured on 2004 January 2 within GO program C026 (P.I.: TL), while a second, shorter series of exposures (4.25 ks) was secured by JWK on 2004 December 19 within the FUSE photometric calibration program M102. Table 1 summarizes these spectroscopic observations, together with those secured for this project with other instruments. Data were reduced using the pipeline software CalFUSE (version 3.2.1). A detailed discussion of CalFUSE 3 is presented by Dixon et al. (2007). The individual exposures were coadded for segments A and B for the four channels (SiC1, SiC2, LiF1 and LiF2) individually. To carry out this procedure, we use the publicly available program FUSE_register written by Lindler (2001) together with scalar weights based on the exposure times. The eight weighted segments were then coadded with the use of a linear interpolation between the spectra in order to produce a final spectrum covering the whole FUSE spectral range. Figure 1 shows the whole FUSE spectrum of PG 0112+104 that was obtained by merging the SiC1B, LiF1A, SiC2B, LiF2A, and LiF1B segments. For the spectral analysis, we combine the segments that provide the best resolution after accounting for the small wavelength shifts between them. In all cases, the noise level varies throughout the spectrum. This is due to the significant change in the effective area of the channels with wavelength, which results in variations in the signal-to-noise ratio. In addition, the number of segments covering a given spectral region is a function of wavelength.

When searching for additional stellar lines, like C III $\lambda 977$ and potential O I, N I, and N II transitions, it is necessary to extract the night-only data, because these lines can be blended with strong emission lines coming from the terrestrial day airglow (see Feldman et al. (2001)). The night-only data are obtained by reprocessing the

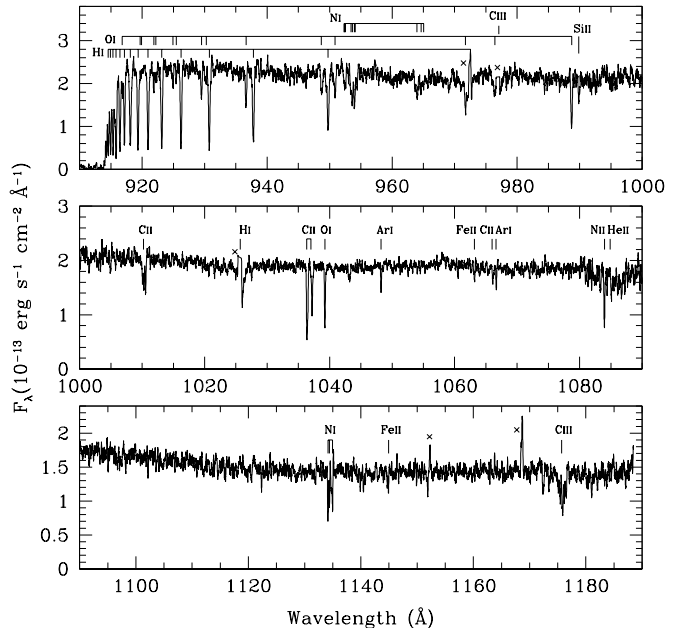


FIG. 1.— FUSE spectrum of PG 0112+104. The spectrum is obtained by merging the SiC1B, LiF1A, SiC2B, LiF2A, and LiF1B segments. The interstellar H I, N I, N II, O I, Si II, Ar I, and Fe II lines are labelled, as are the observed photospheric C II and C III transitions. The symbol x indicates geocoronal emission lines, except for the C III line at 977 Å that originates from scattered solar emission. raw data with the keyword DAYNIGHT set to NIGHT. In this way, the FUSE pipeline processes only data that were taken during the night. That subset amounts to 66 % of the original data secured.

2.2. FOS and GHRs data

Medium-resolution FOS red digicon data of PG 0112+104 can, when combined with medium-resolution GHRs data, be used to construct an energy distribution which replaces the low signal-to-noise data secured many years ago with the IUE satellite and repeatedly analyzed since (Liebert et al. 1986; Thejll et al. 1991; Castanheira et al. 2006).

The FOS data were acquired through the large (3.7" × 1.3") aperture with the red G190H and G270H dispersers, and cover the region between 1571 and 2311 Å, and between 2222 and 3277 Å at a resolution $\lambda/\Delta\lambda = 1300$. This corresponds to $\sim 1 - 2$ Å through our wavelength range. These data were complemented with medium-resolution GHRs data secured through two exposures with the G140L grating and acquired at a spectral resolution of ~ 0.65 Å (image number *z3eu0106p* in the 1136–1422 Å range and *z3eu0107p* in the 1389–1675 Å range). At $\lambda\alpha$, our GHRs data are of lower quality than those secured at better spectral resolution (~ 0.08 Å) by Provencal et al. (2000). These data, a log of which is given by Provencal et al. (2000), were retrieved from the MAST archives. The concatenated medium-resolution data are displayed in Figure 2.

2.3. Optical spectrophotometry

Two blue optical spectra of PG 0112+104 were secured over a time span of 18 years (see Table 1 for a summary of

TABLE 1
SUMMARY OF FUV, UV, AND OPTICAL SPECTROSCOPIC OBSERVATIONS.

Program ID	Date	Grating	$R \equiv \lambda/\Delta\lambda$	Wavelength (\AA)	Exp. Time (s)	Instrument
C0260301	Jan 02 2004	...	18,000	905–1187	22899	<i>FUSE</i>
M1020101	Dec 19 2004	...	18,000	905–1187	4250	<i>FUSE</i>
Z3EU0106P	Nov 15 1996	G140L	2000	1136–1422	653	<i>HST</i> /GHRS
Z3G70207T	Dec 02 1996	G160M	15,000	1196–1234	5658	<i>HST</i> /GHRS
Z3G60205M	Nov 14 1996	G160M	17,000	1316–1353	3699	<i>HST</i> /GHRS
Z3EU0107P	Nov 15 1996	G140L	2300	1389–1676	1197	<i>HST</i> /GHRS
Y3EU0103P	Nov 15 1996	G190H	1300	1571–2311	480	<i>HST</i> /FOS
Y3EU0104P	Nov 15 1996	G270H	1300	2222–3277	160	<i>HST</i> /FOS
...	Jul 19 1991	600(1)	700	3750–5100	2100	2.3 m/B & C
...	Nov 23 2009	600(1)	600	3200–5300	1200	2.3 m/B & C
...	Sep 29 1999	KPC 18C	2200	5600–7400	2400	4 m/R-C
...	Feb 24 2000	KPC 18C	2200	5600–7400	1800	4 m/R-C

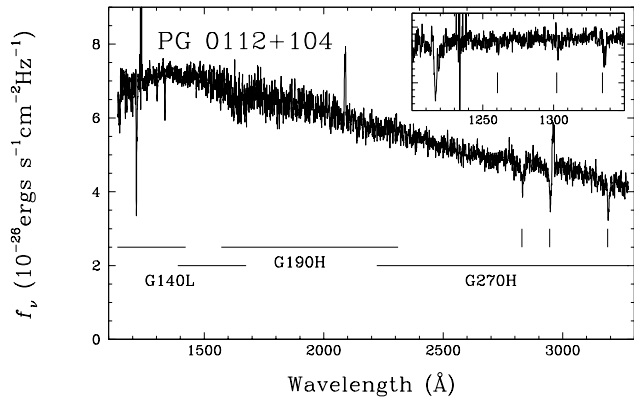


FIG. 2.— Concatenated medium-resolution GHRS and FOS data for PG 0112+104. The data have been smoothed with a 10-point filter. The ranges of the two exposures through the G140L grating on the GHRS and of the two FOS exposures with the red G190H and G270H dispersers are indicated. The three tick marks in the G270H range show the location of strong He I features, while the spikes near 2090 \AA and 2960 \AA appear to be due to improper accounting for counter overflow. The box features an unsmoothed blowup of the 1200–1350 \AA GHRS G140L region, where the H I $\text{L}\alpha$ line as well as the resonant interstellar Si II $\lambda 1260$, O I $\lambda 1302$, and C II $\lambda 1334$ lines are located. The locations of the last three are indicated by tick marks. The four spikes in the 1230–1240 \AA range appear to be associated with an on-board memory problem.

our observations). PG 0112+104 initially belonged to a sample of over 100 DB stars observed over several years in the blue optical region at the Steward Observatory 2.3 m Bok telescope. This sample formed the observational basis for the work of Beauchamp (1995). The instrumental setup includes a Boller & Chivens Spectrograph, a 4.5 arcsec slit, and a 600 l mm^{-1} grating in first order. Together with a 800×800 TI or a 1200×800 Loral CCD, this combination provides coverage of the $\sim 3750 - 5100$ \AA region at an intermediate resolution of ~ 6 \AA . The PG 0112+104 spectrum was characterized by a S/N ratio of 120. More recently, a new observation of PG 0112+104 with the same telescope was secured specifically for this paper. The new data are entirely consistent with the older spectrum secured in 1991, and have the added feature that an annoying instrumental glitch present in the older data near 3950 \AA has been removed.

PG 0112+104 was also included in the sample of stars observed at H α and analyzed by Hunter et al. (2001). The red spectroscopy was secured during two runs at the

KPNO 4 m Mayall telescope equipped with the Ritchey-Chretien Focus Spectrograph, UV Fast Camera, and T2KB CCD. The data from both runs were later combined. Coverage extends approximately from 5600 \AA to 7400 \AA , at a resolution of ~ 3 \AA . A S/N ratio of ~ 90 was achieved. The blue and red spectra are displayed together in Figure 3.

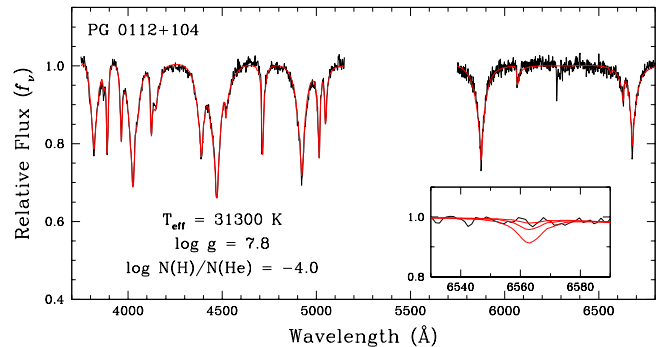


FIG. 3.— Blue and red spectra for PG 0112+104. The optical spectrum of that star shows only lines associated with the He I ion. The features near 6250 \AA are due to night-sky lines. Superposed in red is our fit at the optimal parameters discussed in the text. The insert shows the comparison of our predicted H α profiles for hydrogen abundances of $\log N(\text{H})/N(\text{He}) = -4.0, -3.5,$ and -3.0 .

2.4. High Speed Photometry

High speed photometry was obtained by GF and S. Charpinet on 2002 July 14 UT with LAPOUNE, the portable Montréal 3-channel photometer on the CFHT 3.6 m reflector. The instrument uses three Hamamatsu R647-04 photomultiplier tubes to measure simultaneously the target star, a reference star, and the sky. The light curve of slightly over an hour long (3650 s) was obtained under excellent photometric conditions, and consists of 365 points sampled every 10 s. Our light curve is shown in Figure 4.

3. MODEL ATMOSPHERE AND SYNTHETIC SPECTRUM CALCULATIONS

Our analysis is based on our updated grid of white dwarf models described in Tremblay & Bergeron (2009) in which we have incorporated the improved Stark profiles of neutral helium of Beauchamp et al. (1997).

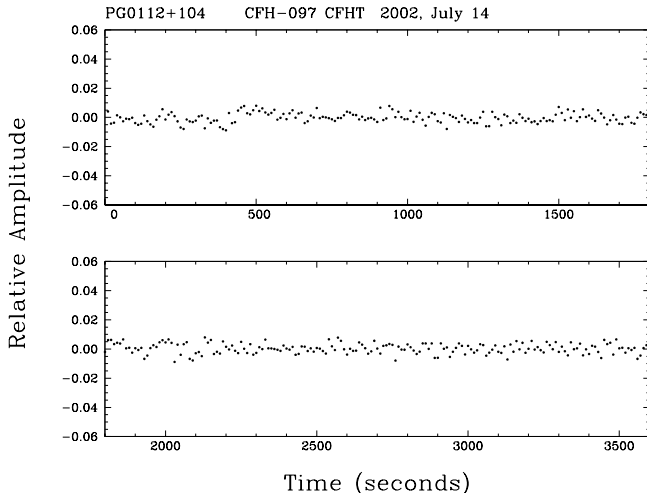


FIG. 4.— Light curve of PG 0112+104 obtained at the CFHT. The observation lasted 3650 s, and the sampling time was 10 s.

In the context of DB stars, these models are comparable to those described by Beauchamp (1995) and Beauchamp et al. (1996), with the exception that at low temperatures ($T < 10,800$ K), we now use the free-free absorption coefficient of the negative helium ion of John (1994), but this should have no effect on the analysis of PG 0112+104 (as discussed further below). Our models are in LTE and include convective energy transport within the mixing length theory. As in the analysis of Beauchamp et al. (1999), we use here the parameterization described as $ML2/\alpha = 1.25$. Synthetic spectra based on these models were used for the $L\alpha$ and optical spectra analyses.

In addition, several calculations were also carried out with TLUSTY and SYNSPEC, the publicly-available model atmosphere codes developed by I. Hubeny and one of us (TL) (e.g., Hubeny & Lanz 1995), which were also used in the analysis of Provencal et al. (2000). Specifically, we used these codes for the determination of the carbon abundance and to set the upper limits on other heavy elements (see § 5.5 below) as well as to reassess the importance of NLTE effects in DB stars (see § 4 below). While the standard parameterization of the convective efficiency within the mixing length theory included in TLUSTY corresponds to that described by Mihalas (1978), we have modified our version to be able to consider alternative efficiencies.

4. THE IMPORTANCE OF NLTE EFFECTS IN DB STARS

In their analysis of HST observations of helium-atmosphere white dwarfs, Provencal et al. (2000) suggest that NLTE effects in the continuum of DB stars might be significant and deserve consideration in their analysis. Their Figure 3 shows, in particular, deviations at the level of 9 % near 1500 Å, and at the level of 4 % near 4000 Å, between emergent fluxes from a LTE model and those of a NLTE model, both computed with TLUSTY at $T_{\text{eff}} = 25,000$ K. This comes a bit as a surprise since the early investigations of both Kudritzki (1976) and Wesemael (1981) suggested that NLTE effects in the continuum were negligible even at effective temperatures considerably higher than that of Provencal et al. (2000). Dreizler & Werner (1996) also

justified a LTE analysis of the DB stars on the basis of the complete absence of NLTE effects in the He I line spectrum at $T_{\text{eff}} = 40,000$ K; NLTE effects in the lines can persist even when continuum NLTE effects are completely negligible (a case in point would be the sharp $H\alpha$ core in cool DA stars). Even more recently, in a re-analysis of hot SDSS DB white dwarfs in the DB-gap, Hügelmeyer & Dreizler (2009) concluded that LTE is a valid assumption for objects with effective temperature below 45,000 K. The result of Dreizler & Werner (1996) and Hügelmeyer & Dreizler (2009) thus appear to confirm the earlier assessment that NLTE effects are negligible for the analysis of DB stars.

Intrigued by the Provencal et al. (2000) claim, which is based on TLUSTY models, we have computed our own NLTE models of DB stars with TLUSTY. The input parameters are identical to those of Provencal et al. (2000), namely $T_{\text{eff}} = 25,000$ K, $\log g = 8.0$, $\log N(C)/N(\text{He}) = \log N(\text{H})/N(\text{He}) = -5.0$, and the parameterization of Mihalas (1978) for the convective flux within the mixing-length theory. We find no observable NLTE effects in the ultraviolet and optical continua at that effective temperature. Furthermore, additional tests suggest that no NLTE effects are apparent in the optical He I line spectrum at 40,000 K and 30,000 K, the highest temperature we considered. This is in complete agreement with the result of Dreizler & Werner (1996) and Hügelmeyer & Dreizler (2009). However we find NLTE effects within ± 2.5 Å of the core of the $L\alpha$ line, which is formed high in the photosphere. We have explicitly checked that these effects have no significant impact upon the analysis we carry out, given that the saturated interstellar profile at $\log N_{\text{H}} = 19.4$ dominates the core of the observed $L\alpha$ profile. We also explicitly verified that the models calculated with small traces of carbon are identical to those without carbon. The abundance of carbon needs to be several orders of magnitude higher, which is ruled out by spectroscopic observations, to have any detectable effect on the thermodynamic structure. Therefore, classical LTE DB atmosphere models are sufficient for determining the effective temperature and the surface gravity of PG 0112+104 from the optical spectra.

5. ANALYSIS

5.1. Determination of the atmospheric parameters from optical data

The analyses of Beauchamp (1995) and Beauchamp et al. (1999) show that the effective temperature determined from the optical spectrum of hot DB stars depends on the hydrogen abundance adopted for the atmosphere, despite the fact that hydrogen may not be directly visible. This is why two effective temperatures, which differ by 200–4000 K, are listed by Beauchamp et al. (1999) for the majority of DB stars: the hotter one was obtained under the assumption of a completely hydrogen-free atmosphere, and the cooler one was obtained under the assumption that hydrogen is present at an abundance slightly below that at which the $H\beta$ line would become visible. In general, thus, the fits to the He I lines in the optical provide a locus of optimal effective temperatures as a function of assumed hydrogen abundance.

The constraints that can be placed on the photospheric

hydrogen abundance thus represent important ingredients in the analysis of hot DB stars. These can be obtained by searching either the $H\alpha$ transition in the red or the $L\alpha$ transition in the ultraviolet. Both techniques have well-known advantages and disadvantages. In rare cases, for example for bright or important objects, both sets of data are available. This is the case for PG 0112+104.

The fits to the older blue optical spectrum of PG 0112+104 by Beauchamp et al. (1999) yielded $T_{\text{eff}} = 31,500$ K, $\log g = 7.82$ for a pure helium composition, and $T_{\text{eff}} = 28,300$ K, $\log g = 7.76$ for a composition with $\log N(\text{H})/N(\text{He}) = -3.0$. This representative abundance was chosen at the time on the basis of a quick look at the newly-acquired GHRS data which appeared to show a fairly strong $L\alpha$ profile. Of course, the profile has since been shown by Provencal et al. (2000) to have a substantial interstellar contribution, and their derived photospheric hydrogen abundance, namely $-4.0 < \log N(\text{H})/N(\text{He}) < -3.5$, is consequently somewhat lower than the nominal value used by Beauchamp et al. (1999).

As an internal check of our updated model grid discussed in § 3, we analyzed this older spectrum using our fitting technique that relies on the nonlinear least-squares method of Levenberg-Marquardt (Press et al. 1986), which is based on a steepest descent method. The model spectra (convolved with a Gaussian instrumental profile) and the optical spectrum are first normalized to a continuum set to unity; this continuum is set in a similar fashion to that described in detail in Liebert et al. (2005) for DA stars. The calculation of χ^2 is then carried out in terms of these normalized line profiles only. Atmospheric parameters – T_{eff} , $\log g$ – are considered free parameters in the fitting procedure; in the case of PG 0112+104 we assume a given value of the hydrogen abundance and compare the predicted $H\alpha$ profile with the observations to set a limit on the hydrogen abundance (see below). Our atmospheric parameters with this old spectrum yields $T_{\text{eff}} = 31,600$ K and $\log g = 7.85$ under the assumption of a pure helium composition, in excellent agreement with the values reported by Beauchamp et al. (1999), which suggests that both model grids for DB stars are entirely consistent.

Since the analysis of Beauchamp et al. (1999), a new blue spectrum as well as spectra covering $H\alpha$ have been secured. Our analysis of this blue spectrum using our pure helium grid yields $T_{\text{eff}} = 31,590$ K and $\log g = 7.82$, in almost perfect agreement with the results obtained with our old spectrum. Our procedure is then to fit this spectrum assuming various hydrogen abundances and compare the predictions at $H\alpha$ with our red spectrum. These comparisons are shown in the insert of Figure 3 for $\log N(\text{H})/N(\text{He}) = -4.0$ (31,320 K, 7.82; this is almost identical to our pure helium solution), -3.5 (30,780 K, 7.81), and -3.0 (29,140 K, 7.78). Since $H\alpha$ is clearly not detected in our red spectrum, we adopt as our final solution $T_{\text{eff}} = 31,300 \pm 500$ K, $\log g = 7.8 \pm 0.1$, and $\log N(\text{H})/N(\text{He}) \leq -4.0$, a hydrogen abundance limit that not is grossly inconsistent with the result of Provencal et al. (2000) based exclusively on the $L\alpha$ profile. Our adopted solution is superposed in Figure 3 on top of the the blue and red spectra.

5.2. Constraint on the hydrogen abundance from the $L\alpha$ profile

When $L\alpha$ observations are available, the contribution of both the geocoronal feature and the interstellar medium absorption must be allowed for. As shown by Provencal et al. (1996) and Provencal et al. (2000) in their pioneering analyses of the $L\alpha$ profile in PG 0112+104, GD 190, and in the prototypical V777 Her star GD 358, this can be done successfully when the saturated core and the broad wings are considered separately. For nearby objects, this allows limits on the photospheric hydrogen content to be placed.

The values of the atmospheric parameters we have secured on the basis of the optical data in the preceding section are likely to be the most reliable in terms of the assumptions underlying our analysis. Nevertheless, other spectral ranges, perhaps less amenable to detailed analyses, can contribute to the overall self-consistency of the analysis. In this spirit, we have investigated the consistency of the $L\alpha$ profile, following the method and technique outline by Provencal et al. (2000) in their original analysis, with our optical determination of the atmospheric parameters of PG 0112+104. The saturated part of the profile suggests a fairly well constrained interstellar hydrogen column density of $\log N_{\text{H}} = 19.4 \pm 0.1$, a value consistent with the results of the initial analysis. The resulting photospheric hydrogen abundance depends on the assumed effective temperature, and — given the importance assumed by the interstellar core — a two-dimensional fit would likely not be significant. We plot, in Figure 5, the match to the overall ISM+photospheric $L\alpha$ profile secured with models at our optically determined effective temperature and gravity. This is done for values of the hydrogen abundance of $\log N(\text{H})/N(\text{He}) = -3.0, -4.0, \text{ and } -5.0$. The two panels display matches secured with values bracketing the optimal column density determined above. The theoretical profiles become less sensitive to the hydrogen abundance for $\log N(\text{H})/N(\text{He}) < -4.0$, and an accurate determination of the hydrogen content from the $L\alpha$ profile seems hardly possible. Suffice it to be said that the value we derive from the optical spectrum is consistent with the limit set from the HST data.

5.3. Transitions of He I and He II

Our FOS data show several members of the He I far-ultraviolet series originating on the 2^3S lower level at $E = 159850 \text{ cm}^{-1}$. Prominent among those are the first members at 3187.74 \AA ($2^3\text{S} - 4^3\text{P}$), 2945.10 \AA ($2^3\text{S} - 5^3\text{P}$), and 2829.07 \AA ($2^3\text{S} - 6^3\text{P}$). These transitions can be seen faintly in some of the better exposed IUE LWR spectra of DB white dwarfs (Holberg et al. 2003). As was done with the $L\alpha$ profile, we can investigate here the rough consistency of our atmospheric parameters with those new features, amenable to a preliminary analysis. In Figure 6, we plot the observed FOS data together with a synthetic spectrum generated with SYNPEC at the values of the atmospheric parameters determined above. While the match to the first two transitions appears quite good, it worsens as we move up the series. This is undoubtedly due to a combination of factors, namely the lack of tabulated electron impact widths for the higher line members and the omission, within SYNPEC, of de-

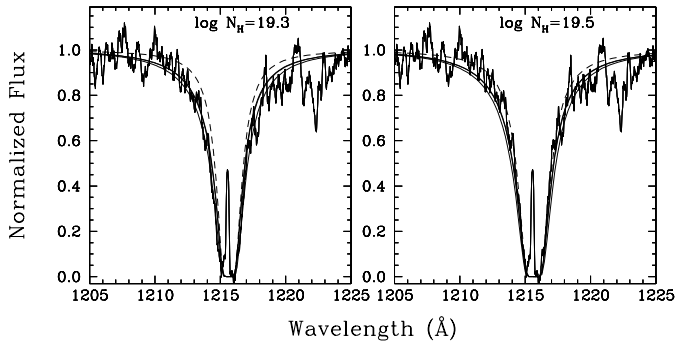


FIG. 5.— Match to the $\text{Ly}\alpha$ spectrum of PG 0112+104 for two labeled column densities, that bracket our best-fitting value, $\log N_{\text{H}} = 19.4 \pm 0.1$. The effective temperature is $T_{\text{eff}} = 31,300$ K, the surface gravity is $\log g = 7.8$, and the hydrogen abundances are $\log N(\text{H})/N(\text{He})$ from -3.0 to -5.0 in steps of 1.0 , from the outside to the inside. The models at -4.0 and -5.0 are nearly on top of each other. In both panels, the innermost short dash profile is the purely interstellar profile.

tailed treatment of the level dissolution as we approach the series limit near 2644 \AA .

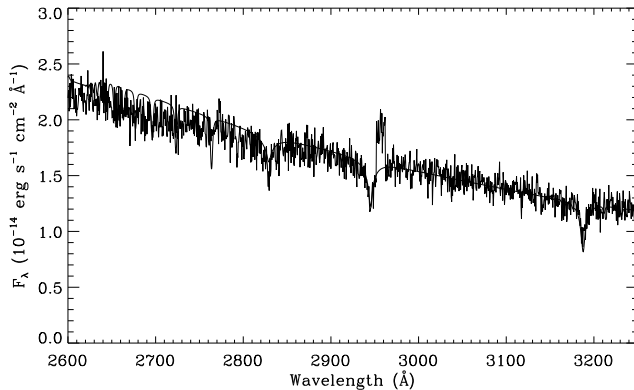


FIG. 6.— Portion of the FOS spectrum showing the He I transitions at 2829.07 , 2945.10 , and 3187.74 \AA that originate on the 2^3S lower level at $E = 159850 \text{ cm}^{-1}$, together with a synthetic spectrum generated by SYNOPSIS.

The S/N ratio of the medium-resolution GHRS data around the He II $\lambda 1640$ transition is unfortunately too low to provide a useful check on the atmospheric parameters of PG 0112+104. Our synthetic spectra do predict a weak He II $\lambda 1640$ transition at this effective temperature, but no meaningful confrontation with the data is possible.

5.4. Energy distribution

The spectral energy distribution of the star provides an additional piece of information. While its slope is, for classical hot DB stars, relatively insensitive to the photospheric hydrogen content and to the surface gravity, it displays some sensitivity to the effective temperature, especially when the energy distribution can be sampled as far as possible in the ultraviolet. While issues related to interstellar reddening and calibration must then be addressed, the matching of the energy distribution of PG 0112+104 affords us with another consistency check on

the adopted values of T_{eff} and $\log N(\text{H})/N(\text{He})$ which cannot be overlooked. Figure 7 displays the energy distribution we have constructed for PG 0112+104. It includes the FUSE data, sampled in 20\AA -wide bins, the HST and GHRS data, sampled in 40\AA -wide bins, as well as the multichannel data, converted to monochromatic flux according to the relation of Greenstein (1976). The match at $V(1.85 \mu\text{m}^{-1})$ defines the solid angle for all the data.

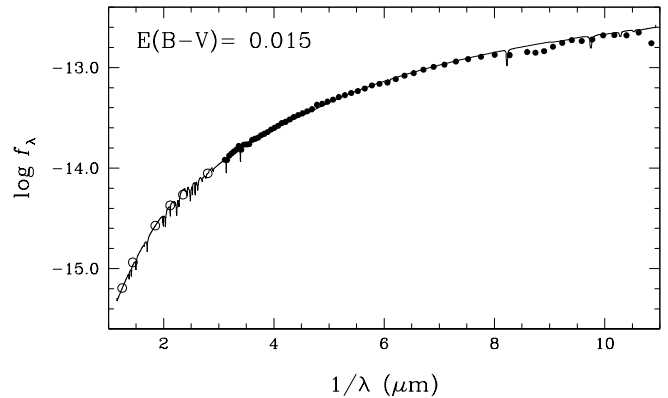


FIG. 7.— The spectral energy distribution of our optimal model (solid line), together with the binned FUSE, GHRS, FOS spectra (filled circles) and the six multichannel magnitudes from Greenstein (1984) (open circles). All data are normalized to the V magnitude. The model parameters are $T_{\text{eff}} = 31,300$ K, $\log g = 7.8$, $\log N(\text{H})/N(\text{He}) = -4.0$. Interstellar reddening is included, with $E(B - V) = 0.015$.

There are, for this object, two modern sets of magnitudes available. The first one, by Greenstein (1984), includes the multichannel V magnitude ($V = 15.36$) together with five MCSP color indices from which six monochromatic magnitudes can be extracted. The second data set, provided by Greenstein & Liebert (1990), lists a full set of 15 monochromatic magnitudes, all simply read off CCD spectrophotometric data. The visual magnitude obtained in that last effort, $V = 15.51$, is a full 0.15 mag fainter than that provided by Greenstein (1984). On the basis of our experience with these data, we restrict our analysis here to the full MCSP data of 1984, which is given on the AB79 calibration scale of Oke & Gunn (1983). Our procedure includes a provision for the contribution of interstellar reddening, as described by the analytic expression for interstellar extinction of Seaton (1979).

Overall, the Greenstein (1984) data leads to a reasonable fit to the energy distribution in the long-wavelength ultraviolet range. The FUSE data, on the other hand, are below the predicted model fluxes. An improved match can be secured by including modest amounts of reddening $E(B - V) \sim 0.03$. This value is consistent with the low column density of neutral hydrogen determined earlier on the basis of the $\text{Ly}\alpha$ profile, namely $\log N_{\text{H}} = 19.4 \pm 0.1$, as well as with the apparent absence of H_2 absorption in the FUSE spectra.

The parallax of PG 0112+104, $\pi = 8.77 \pm 0.55$ mas (Harris 2009), provides an additional consistency check on our analysis. Our preferred match based on the V magnitude of Greenstein (1984) and an interstel-

TABLE 2
CARBON LINE EQUIVALENT WIDTHS AND ABUNDANCES OBSERVED IN FUSE AND GHRS
SPECTRA

Ion	λ (Å)	$\log gf$	g_ℓ	E_ℓ (cm ⁻¹)	E.W. (mÅ)	Abundance	Instrument
C III	977.020	-0.120	1.0	0.000	165.8 ± 13.2	-5.85 ± 0.13	FUSE
C II	1009.858	-0.457	2.0	43003.300	135.3 ± 12.2	-6.13 ± 0.08	FUSE
	1010.083	-0.156	4.0	43025.300			
	1010.371	0.200	6.0	43053.600			
C II	1036.337	-0.611	2.0	0.000	63.7 ± 4.7	-6.03 ± 0.12	FUSE
	1037.018	-0.310	4.0	63.420	82.1 ± 6.2		
C II	1065.891	0.001	6.0	74930.100	23.5 ± 4.9	-6.22 ± 0.14	FUSE
	1065.920	-0.952	4.0	74932.620			
	1066.133	-0.255	4.0	74932.620			
C III	1174.933	-0.468	3.0	52390.750	289.4 ± 19.0	-6.54 ± 0.10	FUSE
	1175.263	-0.565	1.0	52367.060			
	1175.590	-0.690	3.0	52390.750			
	1175.711	0.009	5.0	52447.110			
	1175.987	-0.565	3.0	52390.750			
	1176.370	-0.468	5.0	52447.110			
C II	1323.862	-1.296	6.0	74930.100		GHRS
	1323.906	-0.342	4.0	74932.620		
	1323.951	-0.150	6.0	74930.100		
	1323.995	-1.297	4.0	74932.620		
C II	1334.532	-0.597	2.0	0.000	81.4 ± 8.1	-6.14 ± 0.15	GHRS
	1335.663	-1.295	4.0	63.420	119.7 ± 9.8		
	1335.708	-0.341	4.0	63.420			

lar reddening of $E(B - V) = 0.015$ yields a solid angle of $\Omega \equiv \pi R^2/D^2 = 2.406 \times 10^{-23}$ and a radius of $R = 0.0140 R_\odot$. Here, we have assumed $T_{\text{eff}} = 31,300$ K and a composition with $\log N(\text{H})/N(\text{He}) = -4.0$. We now use the Wood (1992) models with a carbon core, a helium envelope of $10^{-4} M_\star$, and no hydrogen layer, representative of helium-atmosphere white dwarfs. On the basis of these models, we derive $\log g = 7.90 \pm 0.16$ for our energy distribution match, a value consistent with the spectroscopically-determined value.

5.5. Abundances of heavy elements

In addition to interstellar features associated with C II, C III, N I, N II, O I, Si II, and Fe II, the FUSE spectra of PG 0112+104 exhibit many of the photospheric carbon features previously seen in other hot DB stars by Petitclerc et al. (2005) and Desharnais et al. (2008). Five transitions were observed: the C II $\lambda 1010$ triplet, the C II $\lambda 1036$ and $\lambda 1066$ doublets, and the C III $\lambda 977$ line and $\lambda 1175$ complex. Among those, the two components of the C II doublet, $\lambda 1036.337$ and $\lambda 1037.018$, are split since the doublet originates on levels of low excitation energy (ground-state for the blue component, and 63.4 cm^{-1} above the ground state for the red component). Both doublet components thus exhibit well-separated contributions originating in the photosphere and in the ISM. For the other carbon features observed, the energy of the lower levels is high enough to guarantee a photospheric origin. Table 2 lists the transitions uncovered and equivalent widths measured in the FUSE spectra of PG 0112+104. Among the DB stars previously studied with FUSE, EC 20058–5234 — with its effective temperature near 28,000 K — is the closest analog to

PG 0112+104: in that object, Petitclerc et al. (2005) reported the C II $\lambda 1010$ and $\lambda 1036$ doublets, as well as the C III $\lambda 1175$ complex. The C II $\lambda 1066$ doublet was not observed. In addition, the reanalysis by Dufour et al. (2002) of the GHRS spectra of PG 0112+104 secured by Provençal et al. (2000) had shown the presence of the C II $\lambda 1335$ doublet in those data.

We have redetermined individual carbon abundances on the basis of the six transitions of C II and C III observed in the ultraviolet spectra of PG 0112+104. The results are summarized in Table 2 and shown in Figure 8. Our analysis differs little from those carried out earlier (Dufour et al. 2002; Petitclerc et al. 2005; Desharnais et al. 2008). We abstained from carrying out a detailed analysis of the interstellar components in the C II doublets. In the case of the C III $\lambda 977$ line, we analyzed the night-time data of the SiC channels in order to avoid the scattered solar emission contribution. For each transition, the individual uncertainty on the carbon abundance ranges from ± 0.08 dex to ± 0.15 dex. The uncertainties on the carbon abundances take into account uncertainties on the quality of the fit, uncertainties on the oscillator strengths, and uncertainties on the atmospheric parameters ($\Delta T_{\text{eff}} = 500$ K, $\Delta \log g = 0.1$ dex, and $\Delta \text{H}/\text{He} = 0.3$ dex). Table 2 shows that the carbon abundances vary from $\log N(\text{C})/N(\text{He}) = -5.85$ to -6.54 . These two extremes come from the two C III $\lambda 977$ and $\lambda 1175$ lines. Considering all carbon abundances, we obtain a mean carbon abundance of $\log N(\text{C})/N(\text{He}) = -6.15 \pm 0.23$, where the uncertainty is the standard deviation of the measurements. This abundance is consistent with that obtained by Provençal et al. (2000) on the basis of the C II doublet in their GHRS data,

log $N(\text{C})/N(\text{He}) = -5.8 \pm 0.3$ (determined for a slightly cooler effective temperature near 30,000 K), and with the value estimated by Dufour et al. (2002) from the same data, log $N(\text{C})/N(\text{He}) = -6.0$ (for the same effective temperature near 30,000 K).

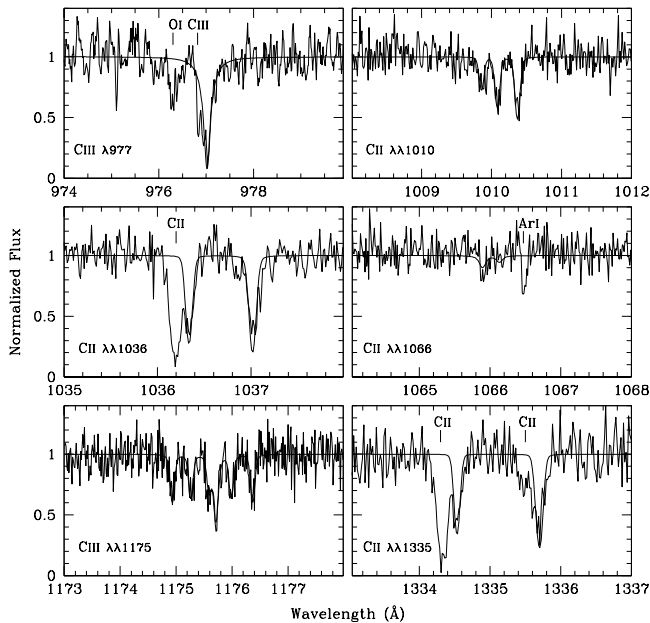


FIG. 8.— Fits to the carbon transitions observed in the *FUSE* and *GHR*S range. The C II $\lambda 1036$ and $\lambda 1335$ features, which originate on low-lying levels, both exhibit a contribution formed in the ISM. Two interstellar O I and Ar I lines are also labelled.

We inspected the *FUSE* spectrum in detail to search for the presence of other elements in the atmosphere of PG 0112+104. No photospheric lines other than carbon were detected. Given that the *FUSE* wavelength range is rich in resonance lines or strong transitions, we were able to estimate abundance upper limits of a dozen elements. Table 3 summarizes our results and shows the lines that we used for determining the upper limits. The upper limits correspond to abundances that are 3σ above the lowest detectable abundances. We measured upper limits of six light elements (N, Si, P, S, Cl, and Ar), five iron peak elements (V, Cr, Mn, Fe, and Co), and one element beyond the iron peak (Pb). The upper limits range from -7.0 to -8.7 . Elements such as oxygen and calcium do not have strong lines in the *FUSE* pass band for a star like PG 0112+104, so no upper limits could be set for these elements.

The problem posed by the presence of carbon in hot, classical DB stars such as GD 358, EC 20058–5234 or PG 0112+104 was addressed by Desharnais et al. (2008), who used the carbon abundance value published by Provencal et al. (2000) (log $N(\text{C})/N(\text{He}) = -5.8 \pm 0.3$) in their discussion. Our updating of the carbon abundance in PG 0112+104 does little to alleviate the problems discussed there and in Petitclerc et al. (2005): “hot” DB stars are too cool for significant radiative element support, but too hot for significant dredge-up or accretion from the ISM.

Fontaine & Brassard (2005) have proposed an attractive scenario to account for the presence of carbon in DB

TABLE 3
UPPER LIMITS ON THE ABUNDANCES OF HEAVY ELEMENTS

Ion	λ (Å)	log gf	g_l	E_l (cm^{-1})	log $N(\text{X})/N(\text{He})$
N III	991.511	-1.317	4	174.400	< -7.0
	991.577	-0.357	4	174.400	
Si III	1113.174	-1.356	5	53115.012	< -8.7
	1113.204	-0.186	5	53115.012	
	1113.230	0.564	5	53115.012	
P III	1003.600	-0.400	4	559.140	< -7.8
S IV	1072.996	-0.829	4	951.100	< -7.2
Cl III	1015.022	0.050	4	0.000	< -8.3
Ar II	932.054	0.120	4	1431.580	< -7.4
V III	1149.945	0.068	10	583.800	< -7.6
Cr III	1033.232	-0.197	9	576.080	< -7.2
	1033.433	-0.259	7	356.550	
	1033.680	-0.245	7	356.550	
Mn III	1108.164	-0.057	12	26824.400	< -7.4
	1111.104	-0.169	12	26851.100	
	1113.186	-0.293	8	26859.900	
Fe III	1122.526	-0.149	9	0.000	< -7.4
Co III	939.062	-0.047	10	0.000	< -7.2
Pb III	1048.877	0.114	1	0.000	< -8.7

stars above 23,000 K. In their view, the observed carbon abundances result from the competition in hot DB stars of efficient downward gravitational settling with a weak stellar wind left over from previous evolution. While there is currently no direct evidence for this wind, its existence is not unreasonable given that signs of mass loss are observed in the PG 1159 progenitors of hot DB stars. The investigation of winds along the cooling track performed by Fontaine & Brassard (2005) is based on fully evolutionary models which include a linear relationship between mass loss and age, with the wind turning off completely by the time a star reaches $T_{\text{eff}} = 20,000$ K. For the hot DB stars, the resulting carbon abundance depends, in the main, on the mass loss rate and is not strongly dependent on the structural parameters of the star (for example, on the helium layer thickness). To account for the abundances summarized by Desharnais et al. (2008), the rates invoked are of the order of a few $10^{-13} M_{\odot} \text{ yr}^{-1}$.

Large amounts of carbon are also found in the so-called hot DQ white dwarfs (Dufour et al. 2007, 2008). These carbon-dominated atmosphere white dwarfs are believed to be the offsprings of DB white dwarfs with very thin helium layers that have experienced a convective mixing episode with the underlying carbon envelope. However, the hot DQ stars are all found at a much lower effective temperatures ($\sim 18,000 - 24,000$ K) than PG 0112+104. It thus appears very unlikely that the carbon observed in the atmosphere of this hot DB white dwarf could be the result of a similar convective transformation caught in its early phase.

5.6. Is PG 0112+104 a True V777 Her Variable?

PG 0112+104 had generally been considered a constant star on the basis high-speed photometry carried out by Robinson & Winget (1983) and Kawaler et al. (1994). Its effective temperature has generally been located in the 27,000 K – 30,000 K range (Liebert et al. 1986; Beauchamp et al. 1999; Provencal et al. 2000; Castanheira et al. 2006), although Thejll et al. (1991) quote a temperature as low as 24,300 K.

Because its effective temperature placed it early on

near the blue edge of the instability strip of the V777 Her variables, high-speed photometry of PG 0112+104 has been carried out on several occasions to search for the non-radial pulsations that characterize the V777 Her stars. Only upper limits on variations were reported. Thus Robinson & Winget (1983) list maximum semi-amplitudes of 0.30 % in the 10 s– 50 s window, of 0.21 % in the 50 s– 200 s window, and of 0.29 % in the 200 s– 1200 s window, while Kawaler et al. (1994) report upper limits on the amplitude of brightness variations of 0.34 %, the later being based on UV data where the amplitudes are expected to be even larger than in the optical.

More recently, however, Shipman et al. (2002) and Provencal et al. (2003) have reopened the debate and suggested, on the basis of 30 h of observing carried out in 2001 October at the McDonald observatory 2.1-m telescope, that the object might be variable, with two periods tentatively identified: $P = 168.98$ s, with an amplitude of 0.083 %; and $P = 197.76$ s, with an amplitude of 0.087 %. The noise level in the Fourier amplitude spectrum is ~ 0.018 %. The periods they infer are consistent with those that characterize known V777 Her stars (100 – 1100 s), but the reported amplitudes are considerably lower than those observed up to now even in the lowest-amplitude V777 Her pulsators, which are ~ 4.6 % (for PG 1351+489 and PG 2246+121).

If the pulsations observed by Shipman et al. (2002) in PG 0112+104 are real, it is unclear to what extent the driving mechanism — and its associated instability strip — invoked for the regular V777 Her stars may be relevant to the variations they observed. While the Shipman et al. (2002) and Provencal et al. (2003) data were considered preliminary, their potentially crucial importance within the context of pulsation theory prompted us to observe PG 0112+104 as a backup object during one of our high-speed photometry run at the CFHT.

As shown in Figure 9, white light brightness variations with amplitudes greater than 0.08 % of the mean brightness of the star can be ruled out in the period window from 20 s to 1800 s, a range that includes all known periodicities in DBV variables. With a noise level of the order of twice that of Shipman et al. (2002), we see no structure at the frequency (5.06 mHz) corresponding to the 198 s period, while a noise peak might be present at the frequency (5.92 mHz) corresponding to the 169 s period detected by Shipman et al. (2002). Our upper limits on the brightness variations in PG 0112+104 are comparable to (even slightly lower than) the variations reported by Shipman et al. (2002), so we cannot confirm their suggested detection. We note in this context that had PG 0112+104 been a normal V777 Her variable, our observations would have revealed it easily.

What is, then, the status of the variations observed by Shipman et al. (2002)? To our knowledge, neither was their preliminary report published in a refereed journal nor was their claim withdrawn. It is assuredly of some significance that PG 0112+104 was not considered a V777 Her star in the recent review of Winget & Kepler (2008). Even more recently, the discussion of the instability strip of the DB stars of Nitta et al. (2009) includes a private communication from J. Provencal stating that “time series observations of this star [PG 0112+104] have not detected any pulsations”. This revised position is in

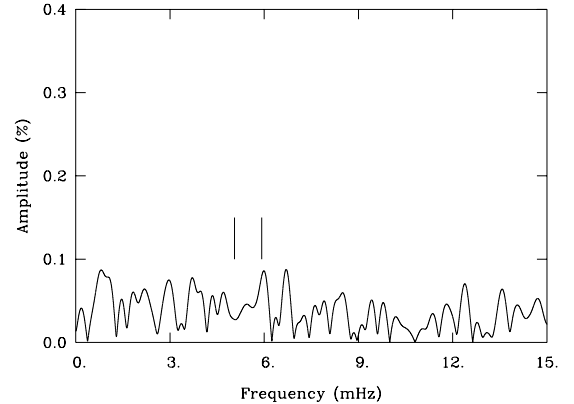


FIG. 9.— Fourier transform of the light curve of PG 0112+104. No peak higher than 0.08 % of the mean brightness is observed in the period window from 20 s to 1800 s.

agreement with our own result, and suggests that PG 0112+104 truly sits above the blue edge of the V777 Her instability strip.

6. CONCLUSIONS

We have provided a comprehensive multiwavelength analysis of the hot DB white dwarf PG 0112+104 based on data largely unexploited up to now. Our analysis yields the following parameters: $T_{\text{eff}} = 31,300 \pm 500$ K, $\log g = 7.8 \pm 0.1$ ($M = 0.52 M_{\odot}$), a hydrogen abundance of $\log N(\text{H})/N(\text{He}) < -4.0$, and an improved carbon abundance of $\log N(\text{C})/N(\text{He}) = -6.15 \pm 0.23$. Since the discovery of several hot DB stars within the SDSS has contributed to the demise of the idea of a true DB gap along the white dwarf cooling sequence, the individual modeling of a single “hot” DB white dwarf may have lost some of its luster. Nevertheless, at $V \sim 15.4$, PG 0112+104 remains one of the few hot DB stars currently amenable to a detailed analysis of the type completed here. PG 0112+104 represents our best object near the transition from nonpulsator to pulsator and our reevaluation of the status of PG 0112+104 as a V777 Her star in § 5.6 underscores the fact that, even for the brightest members, a complete picture of these complex objects is only slowly developing. There are still many aspects about the evolution of helium atmosphere white dwarf that are not completely understood yet, for instance the observed carbon and hydrogen abundance patterns and the exact location of the instability strip. This study brings much needed empirical knowledge about these issues but more work on helium-rich white dwarfs will be needed for a complete understanding of these objects to emerge.

7. ACKNOWLEDGEMENTS

We are grateful to S. Charpinet, R. Lamontagne, D. Paquin-Ricard, and G. Scarpa for their contributions at various stages of this project, to D. Durand and M.R. Rosa for cogent comments on the HST data, to J.L. Provencal for sharing her spectroscopic and model atmosphere results with us along the way, and to H. Harris and to the U.S. Naval Observatory for making the parallax available in advance of publication. PD is a CRAQ postdoctoral fellow and PC was a Canadian representative to the FUSE project supported by CSA under a

PWGSC contract. TL was supported by NASA grant NAG5-12480, and PB is a Cottrell Scholar of the Research Corporation for Science Advancement. This work

was supported in part by the NSERC Canada and by the Fund FQRNT (Québec).

REFERENCES

- Asplund, M., Grevesse, N., & Sauval, A. J. 2005, in ASP Conf. Ser. 336 : Cosmic Abundances as Records of Stellar Evolution and Nucleosynthesis in honor of David L. Lambert, ed. T. G. Barnes III & F. N. Bash, 25
- Beauchamp, A. 1995, Ph.D. thesis, Univ. de Montréal
- Beauchamp, A., Wesemael, F., Bergeron, P., Liebert, J., & Saffer, R. A. 1996, in ASP Conf. Ser. Vol. 96, Hydrogen-Deficient Stars, ed. S. Jeffery & U. Heber (San Francisco: ASP), 295
- Beauchamp, A., Wesemael, F., & Bergeron, P. 1997, ApJS, 108, 559
- Beauchamp, A., Wesemael, F., Bergeron, P., Fontaine, G., Saffer, R.A., Liebert, J. & Brassard, P. 1999, ApJ, 516, 887
- Castanheira, B.G., Kepler, S.O., Handler, G., & Koester, D. 2006, A&A, 450, 331
- Desharnais, S., Wesemael, F., Chayer, P., Kruk, J.W., & Saffer, R.A. 2008, ApJ, 672, 540
- Dixon, W.V. et al. 2007, PASP, 119, 527
- Dreizler, S. & Werner, K. 1996, A&A, 314, 217
- Dufour, P., Fontaine, G., Liebert, J., Schmidt, G. D., & Behara, N. 2008, ApJ, 683, 978
- Dufour, P., Liebert, J., Fontaine, G., & Behara, N. 2007, Nature, 450, 522
- Dufour, P., Wesemael, F., & Bergeron, P. 2002, ApJ, 575, 1025
- Eisenstein, D. J., et al. 2006, AJ, 132, 676
- Feldmann, P. D., Sahnou, D. J., Kruk, J. W., Murphy, E. M. Moos, & H. W. 2001, JGR, 106, 8119
- Fontaine, G. & Brassard, P. 2005, in ASP Conf. Ser. 334 : 14th European Workshop on White Dwarfs, ed. D. Koester & S. Moehler, 49
- Fontaine, G., Villeneuve, B., & Wilson, J. 1981, ApJ, 243, 550
- Fontaine, G. & Wesemael, F. 1987, in I.A.U. Colloquium 95, The Second Conference on Faint Blue Stars, eds. A.G.D. Philip, D.S. Hayes, & J. Liebert (Schenectady: L. Davis Press), p. 319
- Fontaine, G. & Wesemael, F. 1997, in White Dwarfs, eds. J. Isern, M. Hernanz, & E. García-Berro, p. 173
- Greenstein, J.L. 1976, AJ, 81, 323
- Greenstein, J.L. 1984, ApJ, 276, 602
- Greenstein, J.L. & Liebert, J.W. 1990, ApJ, 360, 662
- Harris, H.C. 2009, private communication
- Holberg, J.B., Barstow, M.A., & Burleigh, M.R. 2003, ApJS, 147, 145
- Hubeny, I. & Lanz, T. 1995, ApJ, 439, 875
- Hügelmeier, S. D., & Dreizler, S. 2009, J. Phys.: Conf. Ser., 172, 012048
- Hunter, C., Wesemael, F., Saffer, R.A., Bergeron, P., & Beauchamp, A. 2001, in 12th European Conference on White Dwarfs, eds. J.L. Provençal, H.L. Shipman, J. MacDonald, & S. Goodchild, p. 228
- John, T. L. 1994, MNRAS, 269, 871
- Kawaler, S., Bond, H.E., Sherbert, L.E., & Watson, T.K. 1994, AJ, 107, 298
- Koester, D., Vauclair, G., Dolez, N., Oke, J.B., Greenstein, J.L., & Weidemann, V. 1985, A&A, 149, 423
- Koester, D., Weidemann, V., & Vauclair, G. 1983, A&A, 123, L11
- Kudritzki, R.P. 1976, A&A, 52, 11
- Liebert, J., Fontaine, G., & Wesemael, F. 1987, Mem. Soc. Astr. Italiana, 58, 17
- Liebert, J., Wesemael, F., Hansen, C.J., Fontaine, G., Shipman, H.L., Sion, E.M., Winget, D.E., & Green, R.F. 1986, ApJ, 309, 241
- Liebert, J., Bergeron, P., & Holberg, J. B. 2005, ApJS, 156, 47
- Lindler, D. 2001, in User's Guide, Far Ultraviolet Spectroscopic Explorer. Baltimore: Johns Hopkins University
- Mihalas, D. 1978, Stellar Atmospheres, 2nd edition (San Francisco: Freeman)
- Oke, J.B. & Gunn, J.E. 1983, ApJ, 266, 713
- Oke, J.B., Weidemann, V. & Koester, D. 1984, ApJ, 281, 276
- Nitta, A., Kleinman, S.J., Krzesinski, J., Kepler, S.O. Metcalfe, T.S., Mukadam, A.S., Mullally, F., Nather, R.E., Sullivan, D.J., Thompson, S.E., & Winget, D.E. 2009 ApJ, 690, 560
- Petitclerc, N., Wesemael, F., Kruk, J.W., Chayer, P., & Billères, M. 2005, ApJ, 624, 317
- Provençal, J. L., Shipman, H. L., Riddle, R. L., & Vuckovic, M. 2003, NATO ASIB Proc. 105: White Dwarfs, 235
- Press, W. H., Flannery, B. P., Teukolsky, S. A., & Vetterling, W. T. 1986, Numerical Recipes (Cambridge: Cambridge University Press)
- Provençal, J.L., Shipman, H.L., Thejll, P., & Vennes, S. 2000, ApJ, 542, 1041
- Provençal, J.L., Shipman, H.L., Thejll, P., Vennes, S., & Bradley, P.A. 1996, ApJ, 466, 1011
- Robinson, E.L. & Winget, D.E. 1983, PASP, 95, 386
- Seaton, M.J. 1979, MNRAS, 187, 73P
- Shipman, H.L., Provençal, J.L., Riddle, R., & Vuckovic, M. 2002, BAAS, 200, 7206
- Sion, E.M., Liebert, J., Vauclair, G., & Wegner, G. 1989, in White Dwarfs, ed. G. Wegner (Berlin: Springer), p. 354
- Thejll, P., Vennes, S. & Shipman, H.L. 1991, ApJ, 370, 355
- Tremblay, P.-E., & Bergeron, P. 2009, ApJ, 696, 1755
- Voss, B., Koester, D., Napiwotzki, R., Christlieb, N., & Reimers, D. 2007, A&A, 470, 1079
- Wegner, G. & Nelan, E.P. 1987, ApJ, 319, 916
- Wesemael, F. 1981, ApJS, 45, 177
- Wesemael, F., Green, R.F., & Liebert, J. 1985, ApJS, 58, 379
- Winget, D.E. & Kepler, S.O. 2008 ARA&A, 46, 157
- Wood, M.A. 1992, ApJ, 386, 539